Published August 1, 1995

Spindle Dynamics and Cell Cycle Regulation of Dynein in the Budding Yeast, *Saccharomyces cerevisiae*

Elaine Yeh, Robert V. Skibbens, Judy W. Cheng, E. D. Salmon, and Kerry Bloom

Department of Biology, University of North Carolina, Chapel Hill, Chapel Hill, North Carolina 27599-3280

Abstract. We have used time-lapse digital- and video-enhanced differential interference contrast (DE-DIC, VE-DIC) microscopy to study the role of dynein in spindle and nuclear dynamics in the yeast *Saccharomyces cerevisiae*. The real-time analysis reveals six stages in the spindle cycle. Anaphase B onset appears marked by a rapid phase of spindle elongation, simultaneous with nuclear migration into the daughter cell. The onset and kinetics of rapid spindle elongation are identical in wild type and dynein mutants. In the absence of dynein the nucleus does not migrate as close to the neck as in wild-type cells and initial spindle elongation is confined primarily to the mother cell. Rapid oscillations of the elongating spindle between the mother and bud are observed in wild-type cells, followed by a slower growth phase until the spindle reaches its maximal length. This stage is protracted in the dynein mutants and devoid of oscillatory motion. Thus dynein is required for rapid penetration of the nucleus into the bud and anaphase B spindle dynamics. Genetic analysis reveals that in the absence of a functional central spindle (*ndc1*), dynein is essential for chromosome movement into the bud. Immunofluorescent localization of dynein-β-galactosidase fusion proteins reveals that dynein is associated with spindle pole bodies and the cell cortex; with spindle pole body localization dependent on intact microtubules. A kinetic analysis of nuclear movement also revealed that cytokinesis is delayed until nuclear translocation is completed, indicative of a surveillance pathway monitoring nuclear transit into the bud.

THE dynamic nature of the spindle apparatus during mitosis has been well described in larger eukaryotic systems and is a marvel of natural engineering (Salmon, 1989; Skibbens et al., 1993). One of the emerging principles is that spindle function relies in large part on redundant or overlapping processes. For instance, both kinetochore-based motility and poleward flux of the spindle fibers contribute to chromosome to pole movement (Mitchison and Salmon, 1992). In addition both interpolar spindle pushing forces and astral pulling forces contribute to the separation of spindle poles and chromosomes in anaphase. The analysis of overlapping mechanisms of force generation is difficult in these large cells and reliant on antibody blocking experiments, or single gene knockouts.

Genetic systems are more amenable to dissecting complex interactions and the relationship of distinct pathways that contribute toward the same end can be established. However, the lack of detailed cytological information in many genetic systems preclude a mechanistic understanding of these pathways. In the budding yeast *Saccharomyces cerevisiae*, for example, cells are only 10 μm in size and the metaphase spindle is 1.5 μm in length. Monitoring spindle dynamics at these small dimensions has been difficult. Some success in observing nuclear movements during mitosis has been obtained by staining the nucleus with DAPI (Palmer et al., 1989) or the nuclear membrane with the lipophilic dye, $DiOC_6$ (Koning et al., 1993). In this paper we describe the application of high resolution digitally enhanced and video-enhanced differential interference contrast (DE- and VE-DIC)[1] light microscopy to record spindle and nuclear dynamics in living yeast cells.

We have used these techniques to determine dynein's role in the different stages of mitosis. Genetic studies indicate that dynein plays a profound role in spindle orientation and nuclear migration. Cytoplasmic forms of dynein cloned from fungi include *S. cerevisiae* (Eshel et al., 1993; Li et al., 1993), *S. pombe* (West and McIntosh, 1993), *Aspergillus* (Xiang et al., 1994), *Dictyostelium* (Koonce et al., 1992), and *Neurospora* (Plamann et al., 1994). In budding yeast, binucleates accumulate in the population (Eshel et al., 1993; Li et al., 1993). In filamentous fungi, the mycelia of dynein mutants are almost completely anucleate (as in *Aspergillus*; Xiang et al., 1994) or growth impaired, with nuclei exhibiting extreme clumpiness (seen in *Neurospora*; Plamann et al., 1994).

Address all correspondence to Kerry Bloom, 623 Fordham Hall, CB#3280, Dept. of Biology, University of North Carolina, Chapel Hill, NC 27599-3280. Tel.: (919) 962-1182. Fax: (919) 962-1625. E-mail: Ksb.Fordham@Mhs.Unc.Edu.

1. *Abbreviations used in this paper*: DE-/VE-DIC, digitally enhanced and video-enhanced differential interference contrast; HU, hydroxyurea; SFM, Single Frame Movement; SPB, spindle pole bodies.

Published August 1, 1995

The nuclear migration phenotype is consistent with an interaction between dynein and astral microtubules that extend from the spindle pole bodies into the bud and mother cells. In *S. cerevisiae,* spindle pole bodies (SPBs) direct microtubule assembly and remain embedded in the nuclear envelope throughout cell division. Shortly following spindle pole body duplication, the spindle pole bodies as well as the astral microtubules are oriented to the site of bud growth. Preferential destabilization of the astral microtubules (temperature-sensitive β-tubulin, *tub2-401*) results in malorientation of the spindle, with chromosome separation and nuclear division occurring normally, but confined to the mother cell (Sullivan and Huffaker, 1992). These observations have lead to proposals that dynein's action on astral microtubules may be the primary motive force responsible for spindle orientation and nuclear movement into the bud during cell division.

Dynein may also generate forces responsible for spindle elongation itself. Saunders et al. (1995) have shown that double mutants between dynein and *cin8*, a kinesin-related protein, are inviable, and construction of strains with a temperature-sensitive allele of *cin8* and deletion or disruption alleles of *kip1* and *dhc1* reveal a cooperative role for these three motor proteins in anaphase B spindle elongation. These "synthetic" interactions demonstrate attributes of dynein function not apparent in the dynein mutant alone and point to an additional role of dynein in generating force during spindle elongation.

The application of time-lapse high resolution DE- and VE-DIC microscopy to budding yeast now permits detailed cytological descriptions of dynamic processes within the cell such as spindle assembly, nuclear movements, and organellar segregation. Dynein is required for spindle and nuclear positioning as originally reported, as well as rapid penetration of the nucleus into the bud at the onset of anaphase B and spindle oscillations not previously described in budding yeast.

Materials and Methods

Yeast Strains and Genetic Techniques

The yeast strains used in these experiments are listed in Table I. The construction of the 7.6-kb dynein deletion used in these studies has been previously described (Li et al., 1993). Media, methods of mating, and tetrad analysis were described by Sherman et al., 1986.

Table I. Strains

Strain	Genotype
J178-1D	MATa *ade1 met14 ura3-52 leu2-3,112 his3-11,15*
MCY731	MATα *ura3-52 lys2-801 ade2-101 trp1Δ1 his3Δ200*
KBY5	J178-1D/MCY731 diploid
KBY10	MATa *dhc1Δ7::URA3 ade1 met14 ura3-52 leu2-3,112 his3-11,15*
KBY10u	MATa *dhc1Δ7::ura3 ade1 met14 ura3-52 leu2-3,112 his3-11,15* (5FOA resistant)
KBY11	MATα *dhc1Δ7::URA3 ura3-52 lys2-801 ade2-101 trp1Δ1 his3Δ200*
KBY1	MATα *dhc1::HIS3 ura3-52 lys2-801 ade2-101 trp1Δ1 his3Δ200*
KBY12	KBY10/KBY11 diploid
KBY101u	KBY1/KBY10u diploid
DBY1503	MATa *ndc1-1 ade2 his4-539 ura3-52*
KBY1511	MATa *ndc1-1 dhc1Δ7::URA3 ade 2 his4-539 ura3-52*

Plasmid Construction

The plasmid pDLZ1 (*dhc1-1::lacZ*) was constructed by isolating a 7.5 kb XmaI-BspEI *DHC1* fragment and ligating it to the expression vector YEp357 cut with XmaI to form a fusion protein between *DHC1* and lacZ (Myers et al., 1986). pDLZ2 (*dhc1-2::lacZ*) was constructed by digesting the *DHC1* containing plasmid pYDHC1 (2μ plasmid) with BamHI and ligating to a BamHI lacZ fragment. The integrating *dhc1-3::lacZ* fusion vector pDLZ3 was constructed by cloning a BamHI-PstI fragment into the LacZ integration vector YIp356. Linearization of pDLZ3 with PvuI targets the vector to the *DHC1* locus on chromosome XI.

Nocodazole Treatment

Exponentially growing cultures were treated with 1% DMSO (control) or 1% DMSO with 20 μg/ml nocodazole (Sigma Chem. Co., St. Louis, MO). After 2 h, greater than 80% of nocodazole treated cells were large budded.

Immunofluorescence, DAPI, and Calcofluor Staining

Immunofluorescence staining of yeast cells was performed essentially as described (Pringle et al., 1989). Cells were fixed for 30 min on ice in 3.7% formaldehyde freshly prepared from paraformaldehyde. This fixation did not faithfully preserve astral microtubules. Cells were incubated 20 min in methanol (−20°C) and 30 s in acetone (−20°C) before incubation with antibodies. Microtubules were visualized with the rat anti-α-tubulin antibody YOL1/34 (Accurate Chemical and Scientific Corp., Westbury, NY).

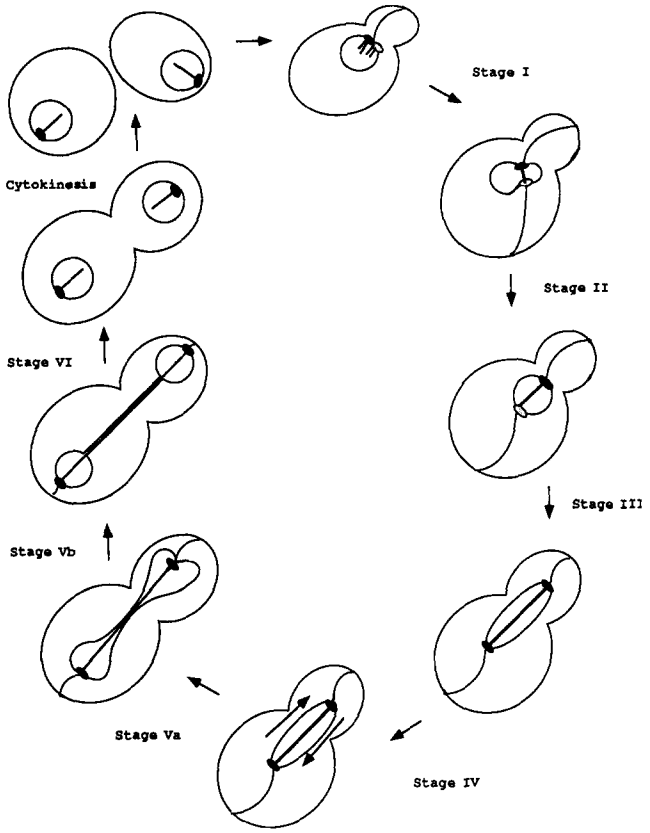

Figure 1. Stages of mitosis in yeast. Six discrete stages in spindle morphogenesis and nuclear division were visualized by DE- and VE-DIC microscopy or indirect immunofluorescence. Structure of the microtubules emanating from duplicated spindle pole bodies are described by Byers and Goetsch (1975). ○, *Spb*; ●, Spb decorated by dyenin-β-galactosidase fusion protein.

Published August 1, 1995

Mouse monoclonal (Promega Corp., Madison, WI) or rabbit polyclonal (Cappel Labs., Cochranville, PA) anti-β-galactosidase antibodies preabsorbed against fixed yeast cells, were used as primary antibodies. FITC-conjugated goat anti-mouse or anti-rabbit and rhodamine-conjugated goat anti-rat (Cappel) were used as secondary antibodies. Cells were incubated in DAPI (1 μg/ml) for 5 min before the addition of mounting medium.

To visualize the nucleus, cells were harvested and fixed in 3.7% formaldehyde for 1 h at 25°C. Fixed cells were washed once with H_2O and resuspended in 1 μg/ml DAPI for 5 min. The cells were washed once with H_2O and mounted in mounting medium. For analysis of the *ndc1* mutants, cells were grown to early logarithmic growth phase at 30°C before shifting to the restrictive temperature of 14°C for 24 h. After DAPI staining cells were incubated in Calcofluor (1 mg/ml) for 5 min and washed five times in H_2O before mounting. To visualize the bud scar and microtubules, cells were fixed in 3.7% formaldehyde for 2 h at 25°C and incubated with Calcofluor (1 mg/ml) for 5 min before spheroplasting. The cells were examined on a Nikon microscope equipped with epifluorescent optics and photographed on Tri-X Pan 400 film.

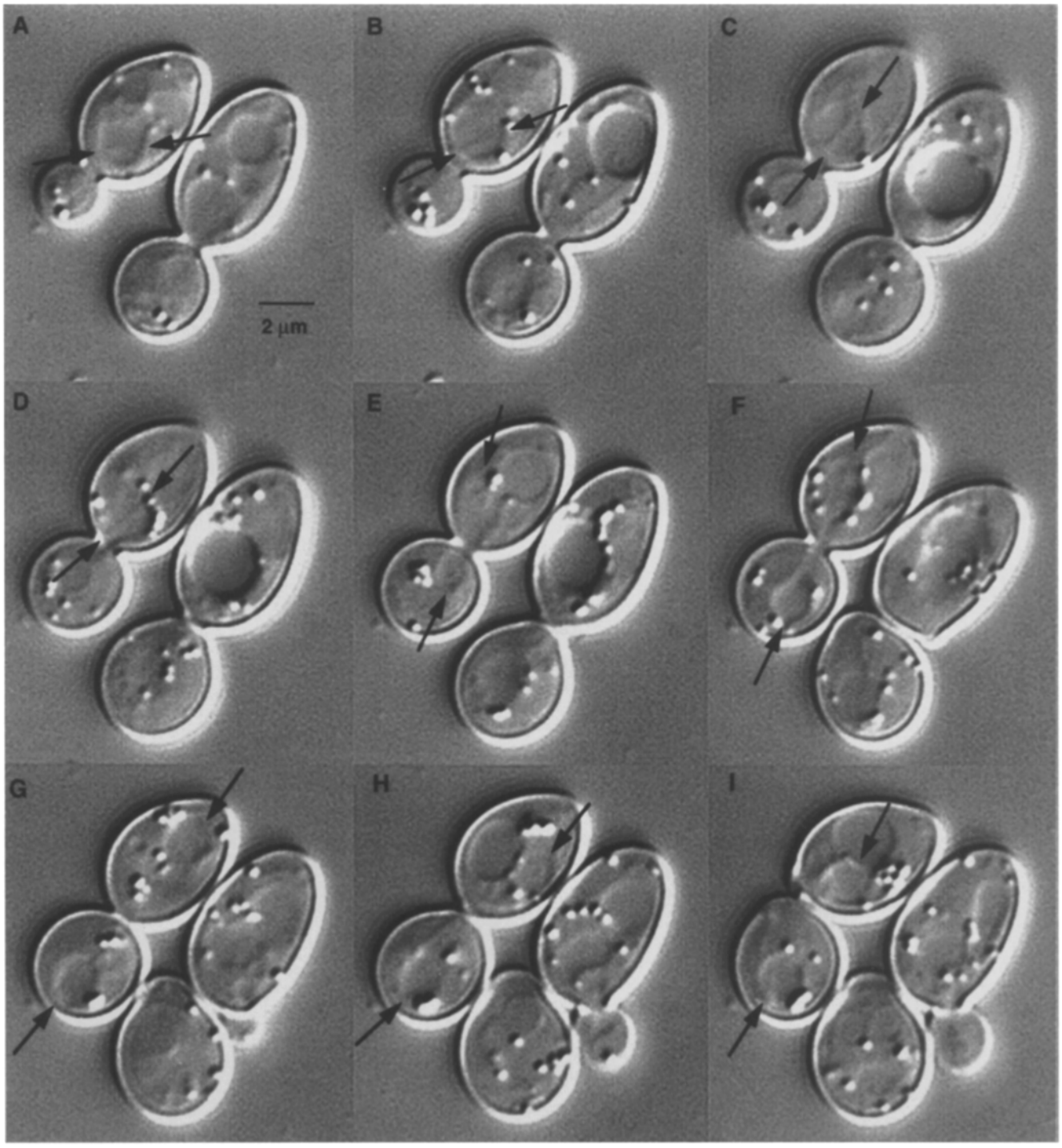

Figure 2. High resolution DE-DIC images of mitosis in a wild-type yeast. A pair of arrows on each frame indicate the spindle orientation. (*A* and *B*) Spindle assembly. A short spindle, not spanning the nucleus is evident. (*C*) Preanaphase spindle bisects nucleus. (*D*) Insertion of the nucleus through the neck. (*E*) Spindle elongation into the bud. (*F*) Bi-lobed nucleus in mother and bud. (*G*) Completion of spindle elongation. (*H*) Nucleus moves from the distal site in the mother to the cell center. (*I*) Cytokinesis.

Published August 1, 1995

Real-Time Analysis of Wild Type and dhc1 Mutants

For high resolution DE-DIC and VE-DIC, cells were spotted onto slabs of 25% gelatin containing YPD (Jones et al., 1993). The increase in refractive index of the surrounding media decreases the contrast from the yeast cell wall and allows visualization of whole cells, including nucleus, spindle, vacuole, and small organelles. All recordings were performed at ambient room temperature ranging from 20–24°C.

Time-lapse VE-DIC microscopy was performed on an optical bench microscope equipped with DIC optics including a Plan 100×/1.25 NA Zeiss objective, a Zeiss 1.4 NA condenser, Zeiss Wallaston prisms; a Zeiss heat-reflecting filter, a heat-cut filter, an Omega (Omega Optics, Burlington, VT) green interference filter (540 nm center wavelength, 20-nm band width) placed before the condenser lens; and illumination from a HBO 100W mercury lamp through an Ellis fiber optic light scrambler (Walker et al., 1990; Skibbens et al., 1993). Images were collected using a Hamamatsu C2400 Newvicon video camera and directly time-lapsed onto a Panasonic TQ2028F OMDR at 240× real time. A PC-controlled Uniblitz (Vincent Associates, Rochester, NY) shuttering mechanism was used to block the illumination beam between exposures.

DE-DIC microscopy was accomplished with a Nikon FXA microscope using a 60×/1.4 NA Plan Apochromat DIC objective and a matching 1.4 NA Achromat condenser, Wallaston prisms, high transmission polarizer and analyzer, and 2× optical projection magnification to the camera. Specimens were illuminated at full objective aperture using a 100W Quartz halogen lamp, ground glass screen, green filters, ND = 32 optical density filter and Uniblitz shutter. Images were integrated for 700 ms on the cooled CCD detector of a Hamamatsu C4880 camera, before being transferred as 12 bit digital files into a Metamorph digital image processing system (Universal Imaging Corp., West Chester, PA). The Metamorph system (see Salmon et al., 1994) controlled time lapse image acquisition at 30-s intervals, image storage on optical disks, image analysis for measurement of spindle pole separation and relative position to the neck of the bud, montaging image frames and printing to a dye sublimation printer (Tektronix Phaser IIsdx; Tektronix, Milan).

A semi-automatic tracking program generated cursors overlaying digi-

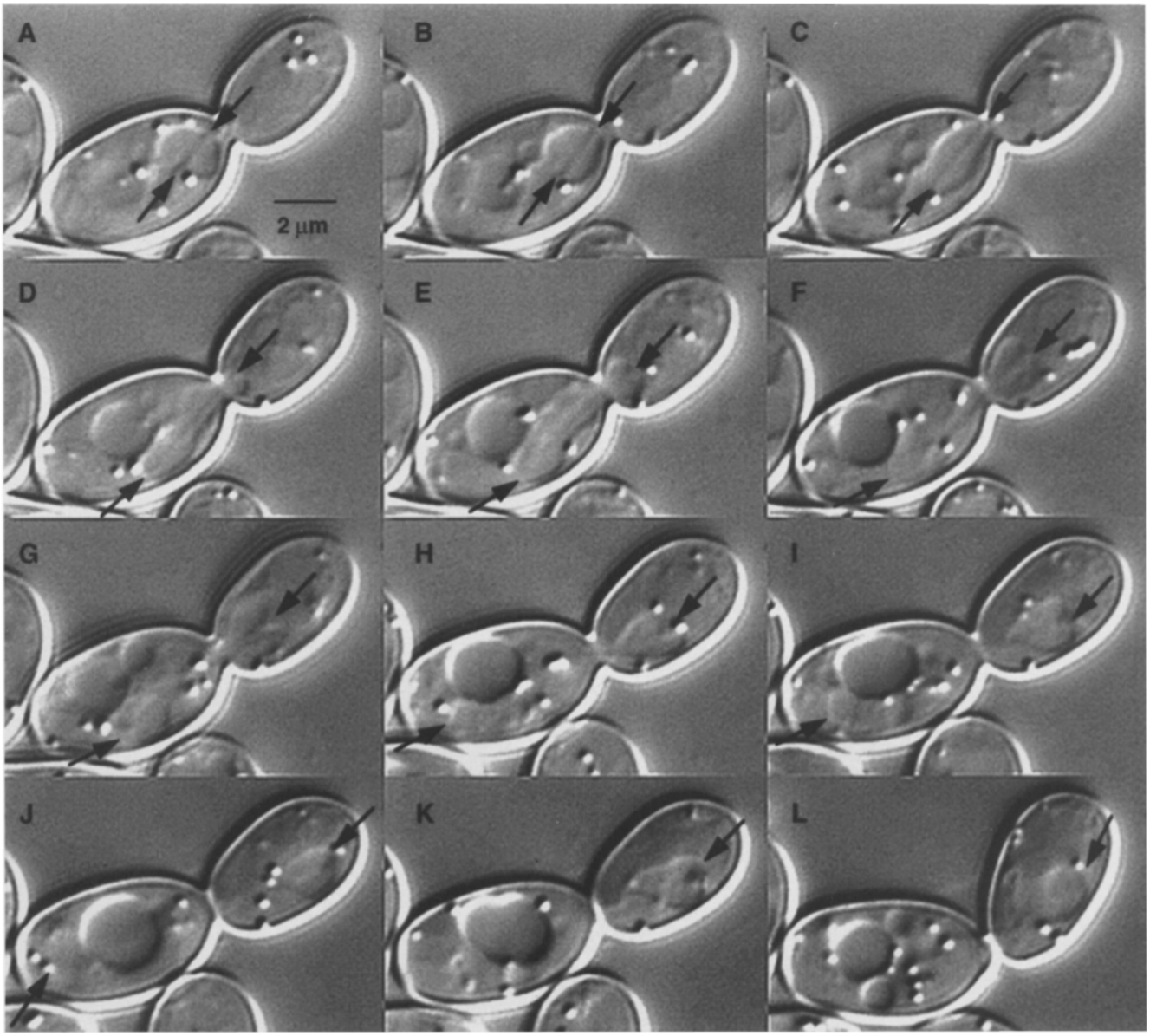

Figure 3. High resolution DE-DIC images of mitosis in a *dhc1* mutant. A pair of arrows on each frame indicate the spindle orientation. (*A*) Preanaphase spindle. (*B–D*) Spindle elongation in the mother cell. (*E–I*) Nucleus becomes "heart" shaped as it moves into the bud. (*J*) Completion of spindle elongation. (*K*) Nucleus moves from the distal site in the bud to the cell center. The nucleus in the mother cell is no longer in the plane of focus. (*L*) Cytokinesis.

Published August 1, 1995

tized images of yeast cells. A Max Video digital image processor (Datacube, Inc., Peabody, MA) and custom software (Walker et al., 1990; Skibbens et al., 1993) was used to accurately track spindle pole bodies or terminal ends of mitotic spindles. Tracking files contained the time interval, OMDR frame number, X,Y coordinates in pixels and Pearson's correlation values for each image tracked. Files were transferred to an in-house motion analysis program, Single Frame Movement (SFM). SFM converts pixel coordinate to distance in microns and generates distance vs. time plots from which regression analysis was performed to obtain velocities.

Alpha Factor Synchronization

Isogenic MATa strains grown to mid-logarithmic phase were arrested with α-factor (Sigma) at a final concentration of 12.5 μg/ml. When >80% of the cells had arrested (schmoo formation), the culture was washed two times with H_2O and resuspended in fresh medium containing 25 mg/ml pronase. At 30-min intervals aliquots were fixed in ethanol and stained with DAPI.

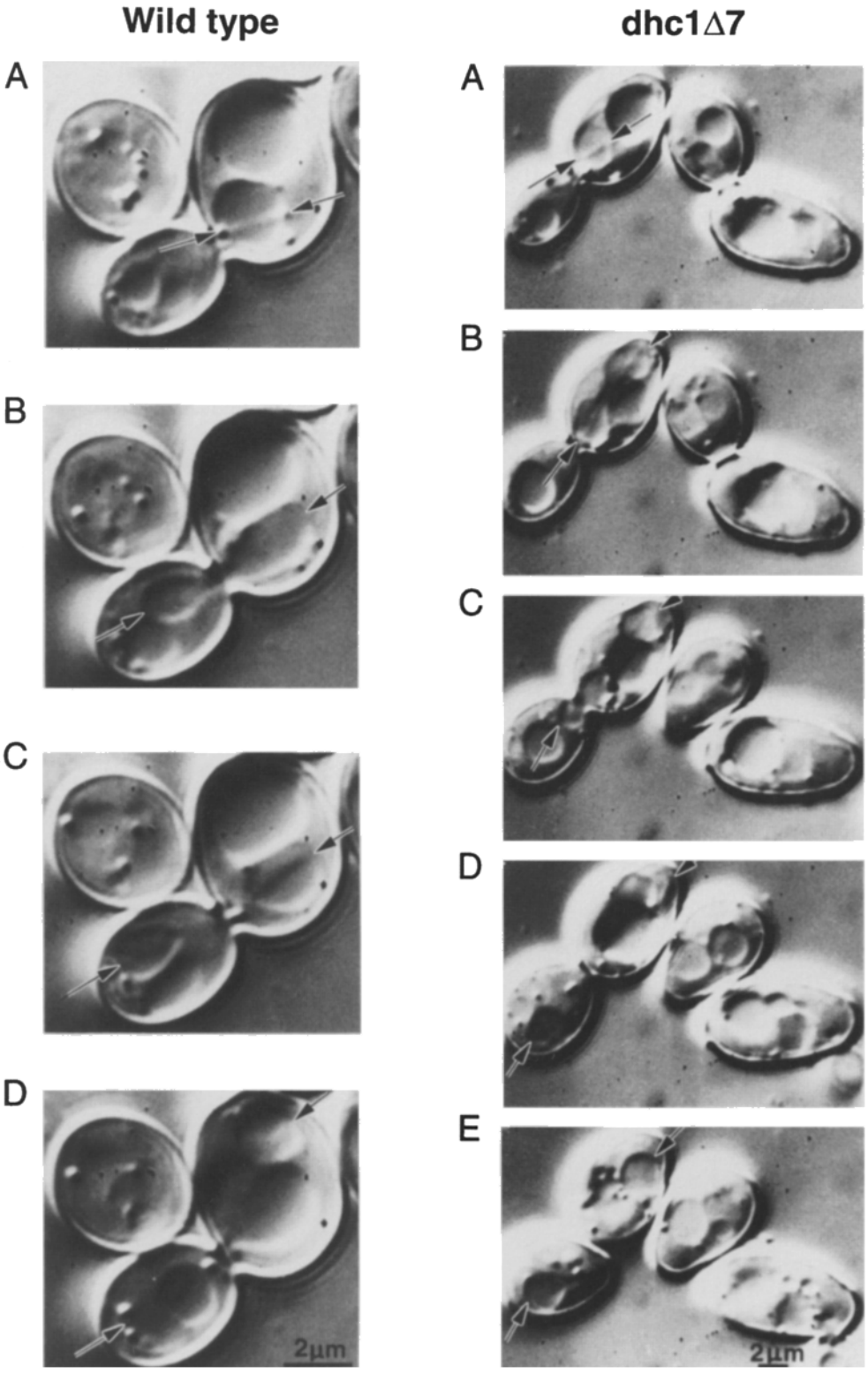

Figure 4. High resolution VE-DIC images of mitosis in wild-type and *dhc1* mutant cells. Wildtype: (*A*) Preanaphase spindle 1.5–2 μm. (*B*) Spindle elongation into the bud. (*C*) Bi-lobed nucleus in mother and bud. (*D*) Separated nuclei. *dhc1* mutant: (*A*) Preanaphase spindle 1.5-2 μm. (*B*) Spindle elongation in the mother cell, nucleus is bi-lobed. (*C*) Nuclear movement into the bud. (*D*) Nuclei move to the distal ends of the cell. (*E*) Nuclei move to the center of the cells and cytokinesis separates the mother and daughter cells. A pair of arrows on each frame indicate the spindle orientation.

Published August 1, 1995

Hydroxyurea Arrest

Isogenic strains grown to early logarithmic growth phase were treated with 0.1 M hydroxyurea (Sigma) to arrest cells in S phase. After 2–4 h (>90% cells large-budded), cells were fixed for immunofluorescence as described above. Greater than 200 cells were counted.

Results

Digital Image Analysis of Yeast Mitosis in Wild Type and Dynein Mutants

We have applied high resolution time-lapse DE or VE-DIC microscopy to examine nuclear division and spindle dynamics in living cells. Six stages in spindle morphogenesis and nuclear division were distinguished and shown diagrammatically in Fig. 1. Each stage represents a distinct step visualized in the DE- and VE-DIC images, or evidenced by quantitative analysis of spindle dynamics described below. An example of DE-DIC images in wild-type cells are shown in Fig. 2.

Stage I. Following spindle pole body duplication, one or both spindle pole bodies migrated through the nuclear envelope to bisect the nucleus. The nucleus was easily discernible and the spindle appeared as a short bar on the side of the nucleus, <1.2 μm in length (Fig. 2, *A* and *B*). One or both spindle poles were occasionally bounded by a refractile particle or vesicle (see Fig. 2 *D*). The spindle constricted the nucleus as the poles separated, and could rotate back and forth 90° on either side of the mother–bud axis. Cells at this stage were small budded (Fig. 2, *A* and *B*), characteristic of early phases in cell cycle progression.

Stage II. Spindle pole separation was complete and a bipolar spindle 1.5–2 μm in length bisected the nucleus (Fig. 2 *C*). During this stage, the spindle remained relatively constant in size over a period of 16 ± 5 min (Fig. 5 *B*, WT $n = 8$, *dhc1* $n = 12$). The nucleus did not appear to be tightly tethered to the neck, exhibiting forward and reverse motion relative to the neck. In addition, the spindle remained free to rotate by 90° obliquely to the mother–bud axis. The spindle pole adjacent to the neck appeared to be destined to the bud. However we could not exclude the existence of rapid spindle "flipping" below the time resolution of these studies. This stage was similar in phenotype to cells arrested by the drug hydroxyurea or *cdc* mutants (*cdc2*, *16*, *20*, and *23*; nuclei with short spindles at the neck of large budded cells, Pringle and Hartwell, 1981), and most likely represents the preanaphase B spindle.

Stage III. The spindle aligned along the mother-bud axis and the nucleus was inserted into the neck (Fig 2 *D*). Then a pronounced spindle elongation occurred (anaphase B), concurrent with the rapid extension of the nucleus into the bud (Fig 2 *E*). Due to the small size of yeast chromosomes and little if any chromosome condensation, anaphase A (chromosome to pole movement) could not be discerned. However onset of anaphase B was quite marked and coincident with movement of the DNA to opposite spindle poles (shown below, see Fig. 7).

Stage IV. The elongated "sausage-shaped" nucleus oscillated over 1–2 μm within the neck, and parallel to the mother and bud axis (Fig. 2 *E*, and diagrammed in Fig. 1). The spindle remained at a constant length, with one pole moving toward the neck accompanied by movement of the opposite pole away from the neck. The spindle often gave the appearance of shortening in length, but upon refocusing was observed to bend away from the original plane of focus at either pole. This bending of the spindle towards the sides of either the mother or bud made it difficult at times to track changes in spindle length.

Stage V. The spindle elongated to its maximal length. Nuclear morphology took a distinctly "hour-glass" shape, with two lobes interconnected by a narrow stem. Elongation of the spindle poles continued until both poles and their nuclear lobes reached a distal position at the ends of the cell (Fig. 2, *F* and *G*).

Stage VI. Finally each of the nuclear lobes moved away from the distal site and became approximately centered in the mother and bud (Fig. 2 *H*). Cytokinesis marked the end of stage VI and the completion of one cell cycle. In time-lapse microscopy, the bud appeared to "snap off" and reposition adjacent to its mother (compare position of bud relative to mother in Fig. 2, *H* with *I*).

The sequence of spindle morphogenesis and nuclear migration in the dynein mutants (*dhc1*) is shown in Fig. 3. Spindle pole body separation and assembly of a bipolar spindle appeared similar in wild type and dynein mutants (Fig. 3 *A*, stages I and II). However the preanaphase B spindle rotations (stage II) were reduced. The spindle was not always aligned along the mother–bud axis, and the nucleus was not inserted into the neck before spindle elongation (Fig 3 *B*). Thus spindle elongation was uncoupled from nuclear migration into the bud as originally reported (Fig. 3, *C* and *D*; see Li et al., 1993; Eshel et al., 1993). The elongated "sausage-shaped" nucleus squeezed slowly into the bud (Fig. 3, *E–H*), often appearing heart-shaped at its

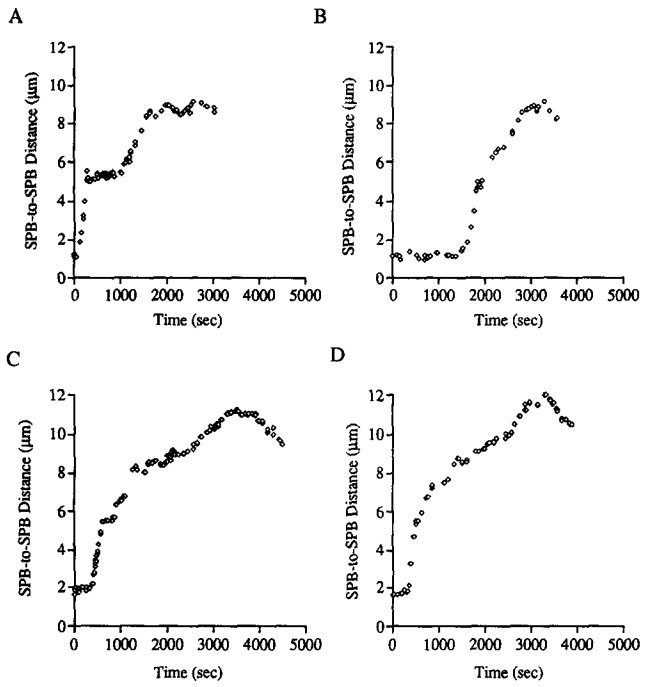

Figure 5. Comparison of the kinetics of mitotic spindle elongation between wild type and *dhc1* mutants. Distances between the SPBs or the ends of the nucleus (μm) are plotted as a function of time (s). (*A* and *B*) Two examples of wild-type cells. (*C* and *D*) Two examples of *dhc1* mutants.

Published August 1, 1995

ends as it traversed the neck. The anaphase B longitudinal spindle oscillations (stage IV) were markedly reduced, if not absent. The nucleus converted into the "hour-glass shape" and the nuclear lobes moved to either end of the cell as in wild type (Fig 3, *I* and *J*). Subsequently, cytokinesis occurred following nuclear positioning toward the center of the cell (Fig. 3, *K–L*).

Quantitative Analysis of Spindle Elongation

A precise analysis of SPB movements was performed for wild type and dynein mutants using a semi-automated tracking system to quantitate spindle morphogenesis and spindle elongation in VE-DIC imaged cells (Figs. 4 and 5). The SPBs or terminal ends of the nucleus were used to track the change in length versus time. The rapid transition to spindle elongation (stage III, Anaphase B onset) could be visualized by the dramatic rise in SPB-SPB distance (Fig. 5 wild type *A* and *B*; *dhc1 C* and *D*). The spindle elongated at a constant rate of 1.08 ± 0.31 μm/min to ~6 μm in length during this stage (Fig. 5). The 6-μm spindle remained constant in length for a variable time in individual cells (Fig 5, *A* and *B*). Further separation to a final length of 8–12 μm continued at a diminished rate (approximately one-third of the initial velocity).

In the dynein mutants the rates of spindle elongation and spindle length were virtually identical to wild-type cells, 1.03 ± 0.25 μm/min and 6 μm, respectively (Fig. 5, *C* and *D*). Thus the initial stages of spindle elongation were not impaired in the absence of the dynein heavy chain. The time to complete spindle elongation (stage V, maximal length 11–12 μm, Fig. 5, *C* and *D*) was significantly delayed, taking one hour in the absence of dynein versus 25–35 min in wild-type cells (compare Fig. 5, *A* and *B* v. *C* and *D* from onset of anaphase B to maximal spindle elongation).

Polarity of Spindle Elongation

The direction of spindle movement was assessed by determining the position of the spindle poles relative to the neck of the budding cell. The neck provided an accurate point of reference in comparing individual cells to each other, and was set as 0 μm. Movement of spindle poles into the bud were plotted as negative values and movement into the mother as positive values (Fig. 6). Immediately preceding spindle elongation, the leading spindle pole abutted the neck (<0.5 μm, Fig. 6 *A*, *open circles*). Spindle elongation proceeded directly into the bud. The entire spindle together with the nucleus oscillated axially within the neck during and after extension of the spindle

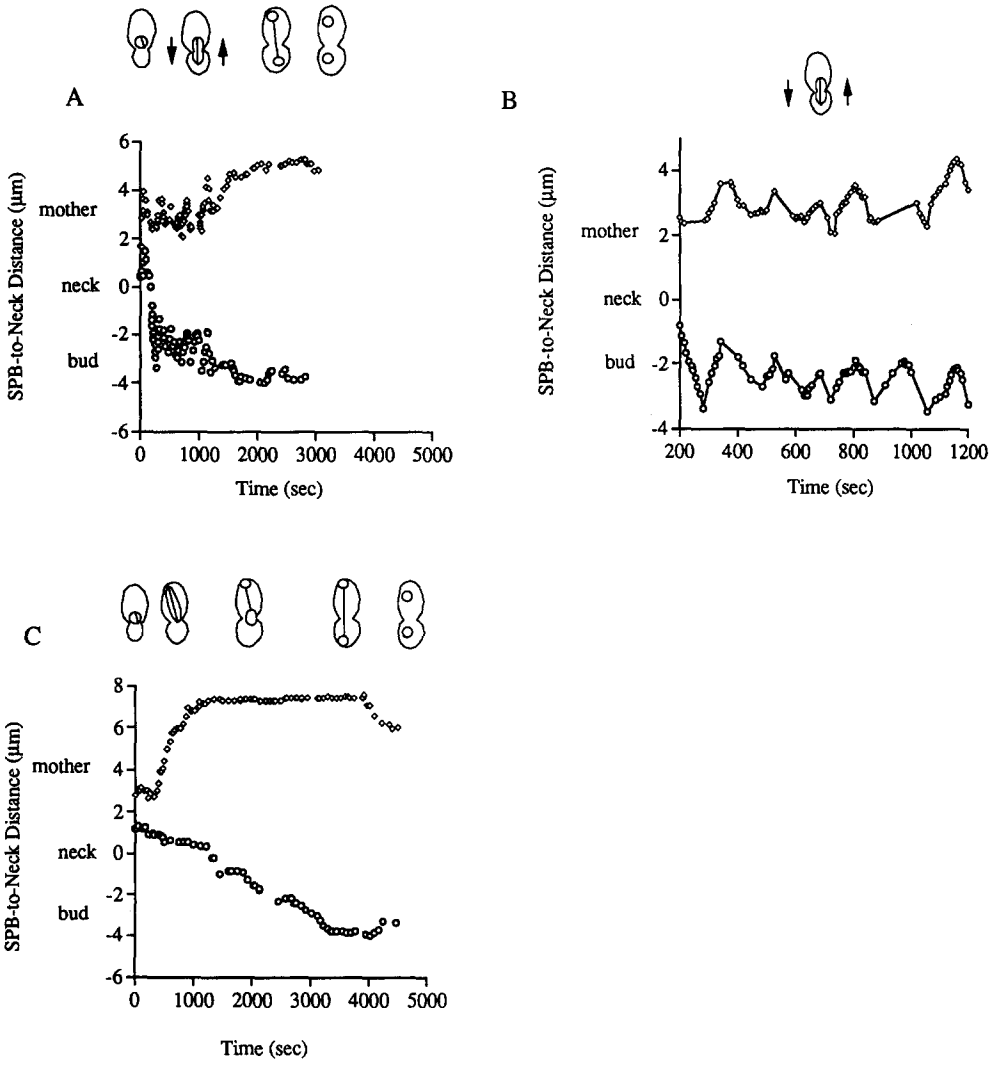

Figure 6. Comparison of the movements of the spindle relative to the bud neck between wild type and *dhc1* mutants. The distance between the neck and each spindle pole body (μm) was measured in cells from Fig. 5 *A* (wt) and 5C (*dhc1*) and plotted as a function of time (s). A schematic representation of the nuclear morphology and position at the different stages is shown above each plot. (*A*) Wildtype 0-neck: positive numbers, mother; negative numbers, bud. Preananaphase spindle at T = 0. (*B*) Wild-type cell with the region 200–1200 s expanded to visualize the coordinated nuclear oscillations back and forth in the neck. (*C*) *dhc1* mutant 0-neck; positive numbers, mother; negative numbers, bud. Preanaphase spindle at T = 0. *Open circles*, SPB proximal to bud; *diamonds*, SPB distal to bud.

Published August 1, 1995

poles. When the time from 200–1,200 s was expanded these oscillatory movements were readily apparent (Stage IV, Fig. 6 *B*), and continued for ~20 min in this cell.

The positional information derived from these SPB-neck plots revealed the dramatic defect in the absence of dynein. Firstly, the nucleus was not positioned immediately adjacent to the neck preceding spindle elongation (0.5 μm wt vs. 1.5 μm *dhc1*, open circles, Fig. 6, *A* and *C*, respectively). Second, spindle elongation proceeded mainly into the mother cell. The spindle pole body away from the neck moved distally in the mother cell. The SPB proximal to the neck did not make further migrations toward the bud at this time (Fig. 6 *C*). Thirdly, the dramatic spindle oscillations characteristic of wild-type cells were noticeably absent in the dynein mutants. The ability to track individual cells revealed that over time, the nuclear lobe proximal to the neck finally moved into the daughter cell and continued to move toward the distal end of the bud (Figs. 4, *C* and *D* and 6 *C*). Depending on the orientation of the spindle at the time of elongation, this period could be fairly short or prolonged. However, spindle elongation occurred in the mother cell in 96% of the cells examined (43/45). This result explains the relatively low fraction of cells (20% binucleate, Fig 7 *B*; Eshel et al., 1993; Li et al., 1993) exhibiting the mutant phenotype. When the spindle was oriented along the mother-bud axis, it elongated into the mother cell, but very rapidly inserted into the bud. These events would be scored as "normal" mitoses when fixed and stained with DAPI. When the spindle was oblique to the mother–bud axis, insertion into the neck was delayed (see below). In both wild type and dynein mutants, the nuclei moved centrally in each cell before cytokinesis as illustrated by the decrease in SPB to neck distance (Fig. 6, *A* and *C*).

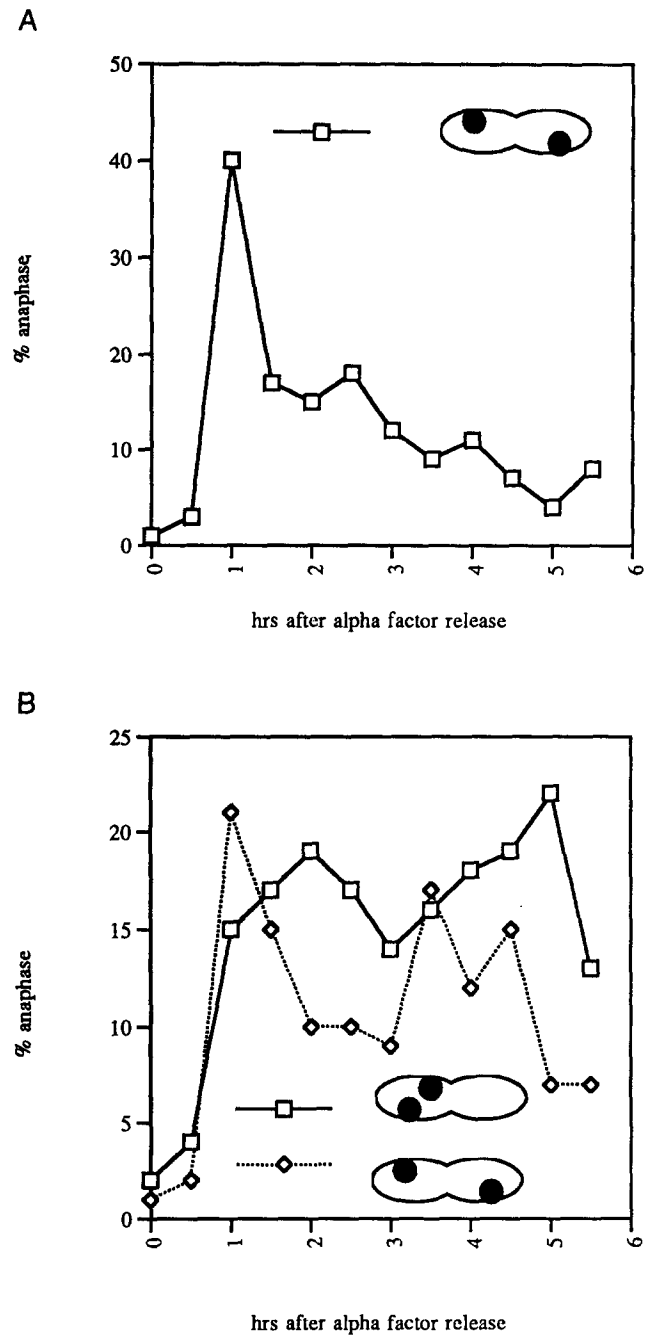

Figure 7. Anaphase B onset in synchronized cells. Cells were synchronized at G1 with alpha factor. At various times after release from the alpha factor arrest cells were fixed and stained with DAPI. Anaphase B was scored as two separated DAPI staining bodies. (*A*) Wild type (*B*) *dhc1* mutant.

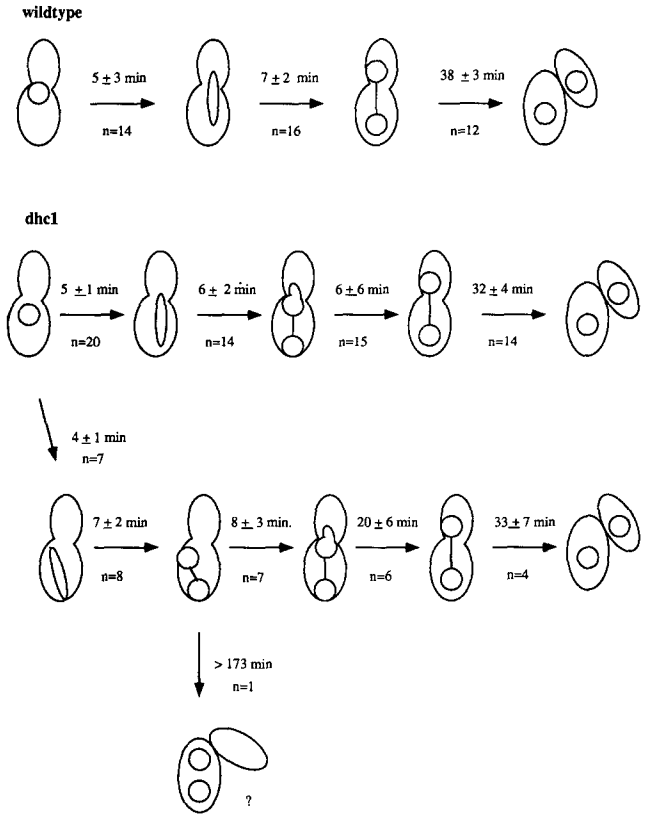

Figure 8. Kinetic analysis of changes in nuclear morphology and spindle dynamics in wild type and *dhc1* mutants. The time between spindle elongation and cytokinesis, seen as cell separation, was determined from the time-lapse videos. In the *dhc1* mutants the time between nuclear migration into the bud and cytokinesis was also determined.

Published August 1, 1995

Timing of Anaphase B Onset and Cytokinesis

The kinetics of anaphase B relative to "start" was examined by synchronizing cells with the mating pheromone, alpha factor and visualizing the appearance of separated DAPI-staining bodies following alpha factor release. By this measure, spindle elongation and chromosome separation occurred at the same time and with the same frequency in wild-type and mutant cells (Fig. 7, *A* and *B*). In wild-type cells, separation of DAPI-staining bodies was coincident with nuclear migration into the bud (40% by 1 h after alpha factor release). Approximately 40% of the dynein mutants also underwent nuclear separation by 1 h after alpha factor release. However in the dynein mutants, half of the events were visualized in the mother cell (Fig. 7 *B*, *squares*) versus mother and bud (Fig. 7 *B*, *diamonds*).

Using the period of anaphase B onset as a landmark, we have determined the kinetics of spindle and nuclear transitions in wild-type and *dhc1* cells. In wild-type cells rapid spindle elongation (stage III) was complete in 5 ± 3 min (~4 μm elongation at a rate of 1.08 μm/min, Fig. 8, *top*, wildtype, n = 14). As described above the duration of rapid spindle elongation was identical in the absence of dynein (4–5 ± 1, Fig. 8, *dhc1 middle* and *bottom*). The transition from a "sausage-shaped" to bi-lobed nuclear morphology took 7 ± 2 min in wild type, and 6–7 ± 2 min in *dhc1*. In the absence of dynein, the transition in nuclear morphology (sausage to bi-lobed) could occur in the neck, or entirely in the mother cell (see Fig 4 *B*, *dhc1*). When the morphological transition took place with one lobe penetrating the neck, complete nuclear migration into the bud was evident in 6 ± 6 min (n = 15, Fig. 8, *dhc1*). When the bi-lobed nucleus was confined to the mother, nuclear migration into the bud was further delayed. Initial penetration of the bi-lobed nucleus took 8 ± 3 min, and complete migration followed in 20 ± 6 min (n = 6, Fig. 8, *bottom*). In one instance the bi-lobed nucleus remained in the bud for over 173 min. Once the nuclear lobe had penetrated the bud, cytokinesis occurred in 32–33 min. The delay in growth of the dynein mutants therefore represents the time to translocate a nuclear lobe into the bud. The large variation from cell to cell represent variations in spindle alignment relative to the mother–bud axis in the dynein mutants. These results confirm the positional defect characteristic of the dynein mutants, and are indicative of additional mechanism(s) that establish the dependency of cytokinesis on nuclear translocation.

Dynein's Role in Nuclear Movement: Hydroxyurea Arrest

One of the more intriguing observations reported in the early analyses of yeast mitosis was the finding that nuclear movement into the bud could precede spindle migration into the bud. Microscopic images obtained by Byers and Geotsch (1975) demonstrated that nuclear material could traverse the neck, while the spindle remained confined to the mother cell. Analysis of our real-time images often revealed the nucleus inserting into the bud ahead of the spindle pole body. To quantify these nuclear movements, cells were treated with hydroxyurea (HU), which blocks DNA replication and arrests cells with the nucleus at the neck of a large budded cell. In wild-type cells containing a single nucleus, the spindle was confined to the mother (100%, n > 300), and a portion of the nucleus could be seen to extend into the bud in ~27% of the cells (Fig. 9, wild type; Table II). In contrast, little penetration of the nucleus into the bud (5%) was evident in dynein mutant cells (Fig. 9, *dhc1*; Table II). Thus in the absence of dynein, nuclear migration to the neck was unimpaired in the HU-blocked cells, but nuclear penetration into the bud was decreased.

Table II. Nuclear Distribution in HU Arrest dhc1Δ7 and Wildtype Cells

								n
	%							
Genotype								
Wildtype	<1	17	47	27	7	0	2	324
dhc1Δ7	1	33	44	5	8	8	1	337

Wildtype and *dhc1* mutant cells arrest as large budded cells in the presence of hydroxyurea. The position of the nucleus relative to the neck and bud was determined in DAPI stained cells. n, cells counted.

Dynein's Role in Nuclear Movement: Nuclear Division Cycle Mutant ndc1-1

The lack of nuclear penetrance into the bud at stage II in the dynein mutants indicated that dynein's site of action

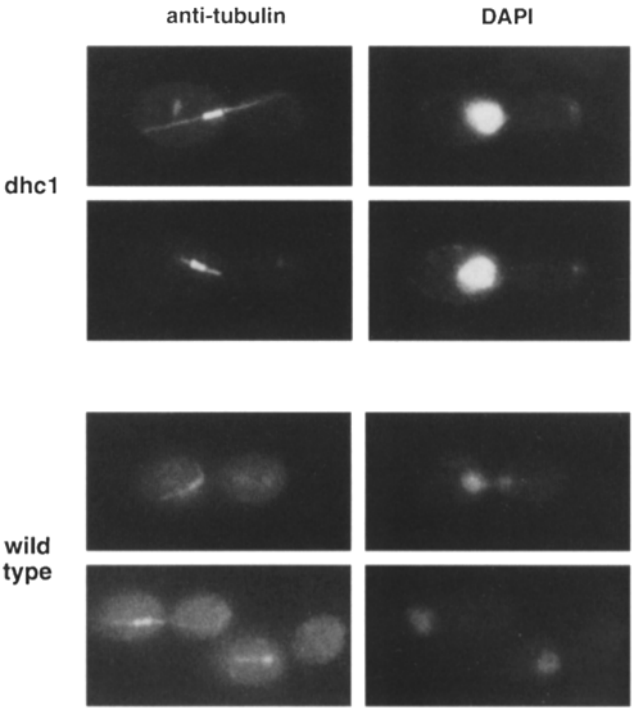

Figure 9. Analysis of nuclear positioning in hydroxyurea arrested cells. Wild type and dynein mutant cells treated with the DNA synthesis inhibitor hydroxyurea arrest with a short spindle confined to the mother cell (intense staining), and cytoplasmic microtubules extending into the daughter cells as seen by anti-tubulin staining. In wild-type cells the nucleus is positioned at the neck. The majority of the staining is within the mother but some DAPI staining extending into the daughter cell is apparent. The nucleus is able to migrate to the neck in *dhc1Δ7* cells but not into the daughter.

Published August 1, 1995

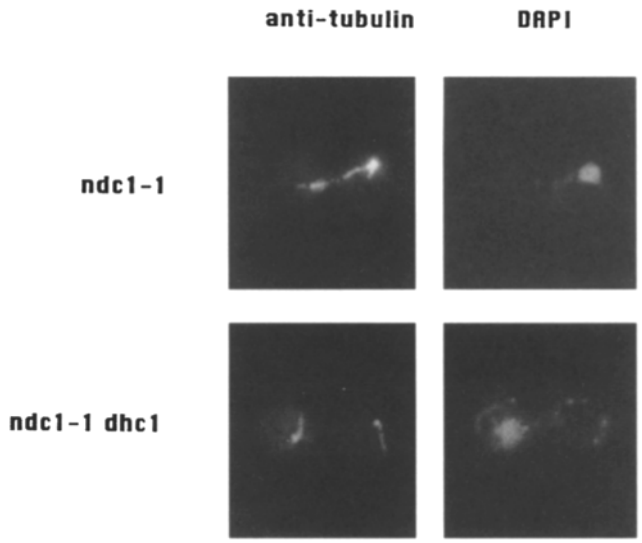

Figure 10. Spindle pole body migration in a *ndc1-1* mutant. *ndc1-1* and *ndc1-1,dhc1Δ7* cells were grown to early logarithmic growth phase at 25°C before shifting to 14°C, the nonpermissive temperature for *ndc1-1*, for 24 h. Cells arrest as large budded cells with a single nucleus. The cells were processed for immunofluorescence as described in the Materials and Methods. *Left* is the anti-tubulin immunofluorescence, *right* is DAPI staining. (*Top*) *ndc1-1*. (*Bottom*) *ndc1-1,dhc1Δ7*.

might be extranuclear. If dynein represented the sole extranuclear force, then elimination of the bipolar spindle (and therefore disruption of spindle forces) should block nuclear translocation into the bud in the dynein mutant. To assess dynein's role in the absence of a bipolar spindle, we constructed double mutants between *dhc1* and the nuclear division cycle mutant *ndc1-1* (Thomas and Botstein, 1986). At the restrictive temperature for *ndc1-1*, the newly synthesized spindle pole body is not correctly deposited into the nuclear envelope. There is a single nucleus with a monopolar spindle and a defective spindle pole body imbedded in the cytoplasmic face of the nuclear envelope (Winey et al., 1993). As shown in Fig. 10, nuclear division was blocked in the *ndc1-1* mutant, and only a single DAPI-staining body could be visualized. To determine whether the chromatin mass remained in the mother or daughter cell, cells were stained with Calcofluor to visualize the birth scar. The mass of the chromatin was found in the mother (62%), bud (14%), or spanning the neck (22%), indicative of nuclear translocation in the absence of a functional central spindle. In the *dhc1*, *ndc1-1* double mutant, the chromatin was observed only in the mother cell (>97%). The defective spindle pole body was able to segregate from the chromatin mass in both *ndc1-1* (Fig. 10, *top* and *bottom*, and Winey et al., 1993) and *ndc1-1*, *dhc1* mutants (Fig. 10 *B*). Thus dynein is essential for chromosome movement, but not spindle pole body movement into the bud in the absence of a functional bipolar spindle. Furthermore, these data reveal the existence of cytoplasmic forces other than dynein that can segregate the defective SPB to the bud.

Intracellular Localization of Cytoplasmic Dynein

We have constructed a series of protein fusions with dhc1p

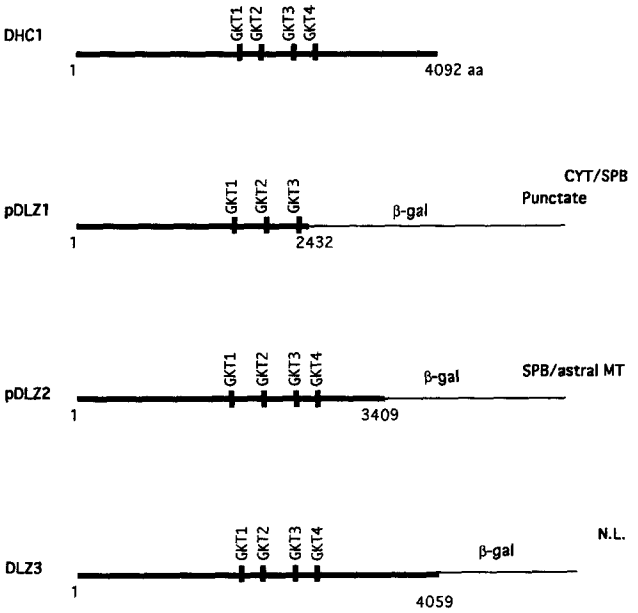

Figure 11. Construction and localization of DHC1-β-galactosidase fusion proteins. Various portions of the *DHC1* gene were fused to the 5′ end of lacZ. The full-length dhc1 protein is depicted at the top with the locations of the putative P loop binding domains denoted by the bars. All fusion proteins are expressed from the DHC1 promoter. pDLZ1 and pDLZ2 are propagated on 2μ plasmids. pDLZ3 is integrated at the DHC1 site on Chromosome XI. The solid bars represent DHC1 sequences present in the fusion protein. The β-gal sequences are equivalent in each. Immunofluorescent microscopy was used to determine the location of the fusion proteins. *Cyt*, cytoplasm; *SPB*, spindle pole body; *NL*, not localized.

and β-galactosidase to determine the intracellular location of cytoplasmic dynein (Fig. 11). An NH_2-terminal fusion, *dhc1-2::lacZ*, containing the first 3409 amino acids of the dynein heavy chain was localized to the single spindle pole in unbudded cells (Fig. 12, *A*). As cells progressed through the cell cycle and assembled short preanaphase spindles (<2 μm), dynein localization remained as a single spot coincident with a single pole body (Fig. 12, *B* and *C*). The SPB closest to the neck was consistently the sole pole decorated by antibody staining in these preanaphase B spindles. The lack of staining of the distal pole provided an internal control that excluded bleedthrough of fluorescence from other channels. The dynein fusion protein was seen to be associated with both poles of the mitotic spindle in cells with elongated spindles (>2 μm; Fig. 12, *D* and *E*) and maintained through the stages of anaphase B (III–V) and late anaphase/telophase (stage VI). At cytokinesis (Fig. 12 *F*) a single spindle pole decorated by the anti–β-galactosidase antibodies could be seen in each progeny cell.

Dynein was also found in association with cytoplasmic microtubules, and as spots in the mother and bud (*dhc1-2::lacZ*, Fig. 13 *A*). In addition, a truncated fusion protein, *dhc1-1::lacZ*, containing only the first three P loop domains (1–2432 aa) was visualized as discrete spots in the bud (Fig. 13 *B*). To address whether the SPB localization seen in Fig. 12 was dependent on the presence of intact cytoplasmic microtubules, microtubule assembly was blocked

Published August 1, 1995

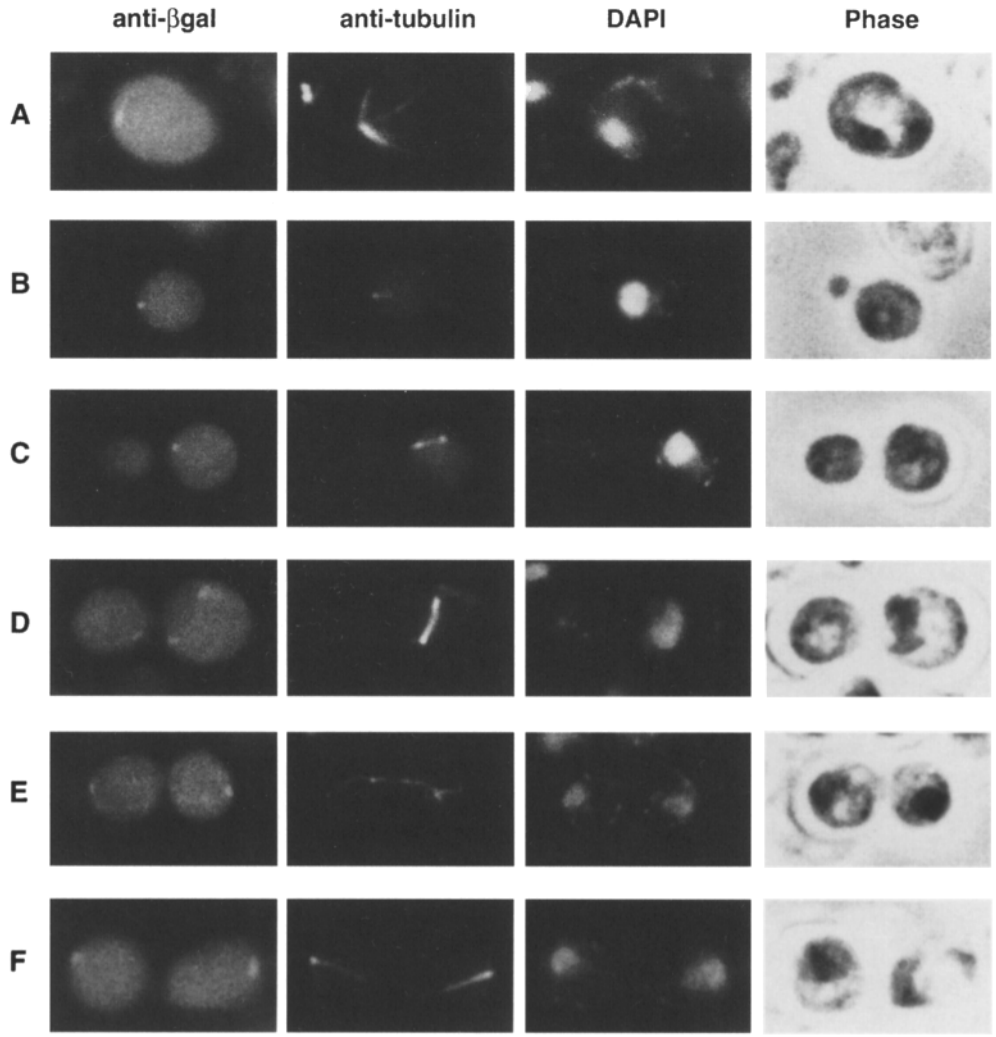

Figure 12. Localization of dhc1-β-Galactosidase during the cell cycle. A wild-type strain containing plasmid pDLZ2 (lacZ fused at codon 3409 of DHC1, *dhc1-2::lacZ*) was analyzed by indirect immunofluorescence. The panels moving left to right are cells stained with anti–β-gal, anti-tubulin, DAPI, and viewed by phase microscopy. Double labeled cells were visualized with FITC-labeled goat anti–mouse or anti–rabbit for β-gal and rhodamine conjugated goat anti–rat for tubulin staining. In single cells (*A*) and cells with small buds containing a pre-anaphase spindle (*B* and *C*) the hybrid protein is localized to a single dot at or near the spindle pole body proximal to the bud. As the spindle elongates (*D*) and the DNA separates (*E*) the hybrid protein is localized at or near both SPBs. At cytokinesis, the spot is observed at the periphery of the mother and daughter cells (*F*).

with nocodazole. Exposure to nocodazole produces rapid disassembly of yeast microtubules and cells arrest growth with a large bud and a single nucleus (Jacobs et al., 1988).

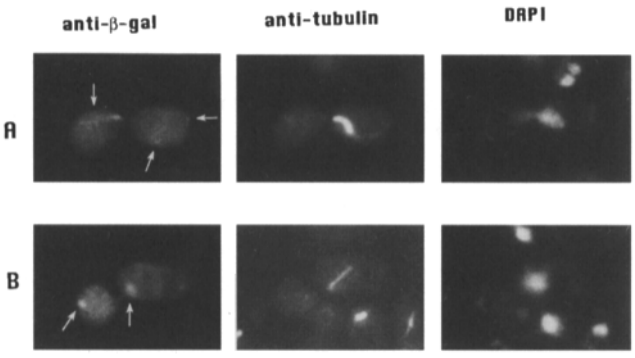

Figure 13. A dhc1-β-gal fusion localizes to cytoplasmic microtubules and as discrete spots in the bud. (*A*) A wild-type strain containing a *dhc1-2::lacZ* plasmid (pDLZ2) was analyzed by indirect immunofluorescence. The dhc1-β-gal fusion localizes to cytoplasmic microtubules. (*B*) A wild-type strain containing a *dhc1-1::lacZ* plasmid (pDLZ1) was analyzed. This dhc1-β-gal fusion localizes to spots in the bud cortex. The panels moving left to right are cells stained with anti–β-gal, anti-tubulin, and DAPI.

In the absence of detectable microtubules, the *dhc1-2::lacZ* staining pattern became more punctate and diffuse, with no propensity for the SPBs (see Table III). The dynein-β-gal fusions were observed in punctate patches in the mother and bud of these cells (diffuse, punctate; no MT staining). Thus the inherent microtubule-based motility of dynein seems likely to be responsible for its association with spindle poles, but not its localization in the cell cortex.

Table III. Dependence of hdhc1::βgal Localization on Microtubules

Anti β-gal: Anti-tub:	SPB MT staining	Diffuse, punctate MT staining	Diffuse, punctate No MT staining	*n*
		%		
DMSO	98	2	0	91
Nocodazole	38	9	53	118

Early logarithmic phase cells containing the plasmid pDLZ2 were treated with DMSO or DMSO plus 20 μg/ml nocodozole. After a 2-h incubation, >80% of the nocodozole-treated cells were large budded. No astral and few intranuclear microtubules were visible by immunofluorescence. In most cases the remnant microtubule structures (Nocodazole 38% + 9%) appeared to be associated with the SPBs. *n*, cells counted.

Published August 1, 1995

Table IV. Dependence of Spindle Events in Selected Mutants

Cell cycle event	Selected mutant or drug treatment						
	Wild type	No astral MTs	*dhc1*	HU	HU, *dhc1*	*ndc1*	*ndc1, dhc1*
Preanaphase, stage I-II							
Nuclear proximity to neck	+	−	+	+	+	?	?
Nuclear penetration into bud	+	−	−	+	−	?	?
Spindle alignment along mother-bud axis	+	−	−	?	?	NA	NA
Anaphase, stage III-V							
Chromatin penetration into bud	+	−	+	−	−	+	−
Segregation of spindle poles into bud	+	−	+	−	−	+	+
Spindle elongation	+	+	+	−	−	NA	NA
Spindle oscillation	+	?	−	?	?	NA	NA
DNA separation	+	+	+	−	−	−	−
Telophase, stage VI							
Recentering of nuclei	+	NA	+	NA	NA	NA	NA
Cytokinesis	+	+	+	−	−	−	−

Results are from this study unless otherwise indicated. No astral MTs: Sullivan and Huffaker, 1992; Palmer et al., 1992; dhc1: Li et al., 1993; Eshel et al., 1993; HU: Pringle and Hartwell, 1981; Palmer et al., 1992; and ndc1: Thomas and Botstein, 1986; Winey et al., 1993.

Discussion

Spindle Dynamics During Mitosis

The application of high resolution DE- and VE-DIC microscopy to living yeast cells provides a kinetic description of spindle dynamics throughout the cell cycle. At least six stages of mitosis can be distinguished. During preanaphase spindle formation (stage I) one or both spindle pole bodies could migrate through the nuclear envelope. One spindle pole remained proximal to the neck, while the other traversed the nuclear envelope. Since the newly synthesized spindle pole is destined for the bud (Vallen et al., 1992), the old spindle pole body is likely to be the motile pole during stage I. The stage II spindle (1.5–2.0 μm) remained constant in length, or elongated very slowly over an ~16-min period. At this stage the spindle appeared fairly rigid and could rotate up to 90° obliquely to the mother–bud axis. Stage III was characterized by rapid linear elongation of the spindle with a velocity of 1.08 μm/min to a length of 6 μm. These rates are consistent with earlier measurements taken from low level DAPI stained cells (Palmer et al., 1989). See-saw movements within the neck (up to almost 2 μm) at a relatively constant spindle length (Stage IV) suggest that when one pole is moving toward the neck, the opposite pole was moving distally. These oscillations could not be generated from within the nucleus, and may correspond to DNA transits previously reported by Palmer et al. (1989). Spindle bending as visualized as movements in and out of the plane of focus, as well as from side to side may be indicative of cytoplasmic MT, SPB or nuclear membrane contacts with cortical sites throughout the cell. Stage V was marked by a slower elongation phase that coincided with the transition from a "sausage-shaped" to "hour-glass" nuclear morphology. Finally, the poles migrated toward the center of their cells before cytokinesis (stage VI). The spindle could often be seen to extend between the bi-lobed nucleus, however the precise time of spindle disassembly and nuclear division could not be determined. Based upon the real-time images, nuclear division occurred shortly before cytokinesis.

Role of Dynein in Nuclear and Spindle Dynamics

The contribution of cytoplasmic dynein to spindle function is summarized in Table IV, along with functional aspects of cytoplasmic microtubules and the central spindle. The first dynein-dependent events were evident in the preanaphase nuclear movements and spindle alignment. The nucleus could migrate proximal to the neck in the absence of dynein, but the spindle did not always align along the mother–bud axis. In addition, nuclear (but not spindle) movements into the isthmus of the neck were not observed in the absence of dynein (Table IV, *Preanaphase stage I-II*, compare *HU* with *HU,dhc1*). The dependency of these early nuclear movements on dynein are likely to reflect interactions between dynein and components of the nuclear envelope, and are indicative of dynein's role in docking the nucleus into a position at the neck where simultaneous translocation and elongation can occur.

In the absence of dynein, the kinetics of Anaphase B were unaffected, however spindle elongation was confined primarily to the mother cell. This result is reminiscent of the phenotype observed when astral microtubule assembly is selectively disrupted (Table IV, *No astral MTs*; Sullivan and Huffaker, 1992). Thus forces from the central spindle, in the absence of astral microtubules are insufficient for nuclear movement into the bud. The temporal deficiency in the absence of *DHC1* indicates that dynein is not functionally unique, as other forces acting on cytoplasmic microtubules are able to compensate for dynein's absence. To assess the relative contribution of cytoplasmic forces, *dhc1*, *ndc1-1* double mutants were constructed. In the absence of a bipolar spindle, movement of the unsegregated chromatin mass into the bud was completely dependent upon dynein (Table IV, *Anaphase, stage III-V, ndc1, dhc1*). However, segregation of the defective spindle pole body into the bud was observed (Table IV, *Segregation of spindle poles into bud, ndc1,dhc1*). Taken together, these data are indicative of additional cytoplasmic forces, and suggestive of a hierarchical array of force producing proteins in the cytoplasm.

Once spindle pole body separation commenced, the spindle oscillations and spindle bending toward the cell

Published August 1, 1995

periphery, that demarcate stage IV are also dependent upon cytoplasmic dynein. The dependence of these events upon dynein is consistent with dynein's role in force production outside the nucleus, and indicate there may be multiple sites of contact between dynein and the cell periphery. In addition, the directionality of pole movement (one toward the neck, the other away from the neck) indicates the stiffness of the central spindle and regulation of extranuclear forces that remains to be addressed.

Assessment and Implications of Dynein::β-gal Localization

It has been proposed that dynein anchored in the cell cortex could pull on the cytoplasmic microtubules and produce force on the spindle and nucleus (Eshel et al., 1993; Li et al., 1993; Schroer, 1994). Localization of dhc1p::β-gal to cortical spots in the bud or mother is compatible with such models. The spindle pole body localization seen in the majority of cells might simply reflect dynein's accumulation at the pole via its inherent minus end-directed motility. This idea is supported by the observation that dhc1p::β-gal SPB association is dependent on intact cytoplasmic microtubules. Similarly, localization of a dynein-activating complex (dynactin) to the centrosome in Rat2 cultured cells is dependent of the presence of microtubules (Paschal et al., 1993). Depolymerization of microtubules with nocodazole changes the distribution of $p150^{GLUED}$ (a component of dynactin) from centrosomal to bright punctate cytoplasmic staining.

Coincident with the onset of anaphase B, dhc1p::β-gal redistributes to both SPBs and appears as cortical spots in the mother and bud. These data are consistent with dynein's proposed participation in anaphase B (Saunders et al., 1995) and in the oscillatory spindle movements observed in living cells. The redistribution to both SPBs or sequential distribution from cortical sites in the bud to the mother suggests that either dynein, or microtubule attachments to the cortex are subject to cell cycle regulation. Since dynein seems to be associated with the pole upon birth of the daughter cell, it must also redistribute from the old to new pole coincident with spindle pole body separation or spindle formation.

Cell Cycle Delay in the Dynein Mutants

The kinetic analysis of structural transitions revealed that the onset of spindle elongation was unaffected in the dynein mutants (Fig. 7). Thus the timing of anaphase B onset was not dependent upon spindle orientation or precise nuclear positioning. However the time to achieve maximal nuclear separation was greatly extended and dependent upon initial nuclear position (Fig. 8). The transition from "sausage-shaped" to bi-lobed nuclear morphology took 6–7 min whether the nucleus spanned the neck (wildtype) or was confined to the mother cell (*dhc1*)(Fig. 8). When the "sausage-shaped" nucleus was close to the neck, the morphological transition to bi-lobed occurred at the neck, and nuclear translocation was only delayed by 6 ± 6 min. If the nucleus was not aligned along the mother–bud axis, and the bi-lobed structure formed entirely in the mother cell, translocation was delayed even further (Fig. 8, *bottom*, 28 min [8 ± 20]), or did not occur at all. It appeared that a great deal of force was required for the translocation event in these instances, and nuclear morphology was a significant parameter in timely nuclear migration. Once a significant portion of the nucleus was inserted into the bud, the time to cytokinesis was 33 ± 7 min (Fig 8, *bottom*). Thus the dynein mutants were delayed in cell cycle progression during the time needed to translocate a bi-lobed nucleus into the bud. It was difficult to distinguish whether nuclear penetration, or complete translocation into the bud was sufficient to initiate the cascade towards cytokinesis. While the mechanism remains to be elucidated, our data reveal that nuclear penetration through the neck initiates a signaling pathway that controls the onset of cytokinesis.

In summary, high resolution DE- and VE-DIC microscopy has delineated at least six stages in spindle morphogenesis and nuclear division. The dynamic range of movements indicate multiple forces that act upon the nucleus, SPB, and astral and nuclear microtubules. Some of these movements are mediated by cytoplasmic dynein and as yet unidentified cytoplasmic force producers. The asymmetric localization of the dynein hybrid protein suggests there is a spatial as well as temporal regulation of dynein activity.

We thank Mark Winey for generously supplying the ndc1 mutants, and K. Tatchell and J. McMillan for communicating JNM1 results.

This work was supported by research grants from the National Institutes of Health General Medical Science (K. Bloom and E. D. Salmon).

Received for publication 17 May 1995 and in revised form 18 May 1995.

References

Byers, B., and L. Goetsch. 1975. Behavior of spindles and spindle plaques in the cell cycle and conjugation of *Saccharomyces cerevisiae*. *J. Bacteriol.* 124:511–523.

Eshel, D., L. A. Urrestarazu, S. Vissers, J.-C. Jauniaux, J. C. van Vilet-Reedijk, R. J. Planta, and I. R. Gibbons. 1993. Cytoplasmic dynein is required for normal nuclear segregation in yeast. *Proc. Natl. Acad. Sci. USA.* 90:11172–11176.

Jacobs, C. W., A. E. Adams, P. J. Szaniszlo, and J. R. Pringle. 1988. Functions of microtubules in the *Saccharomyces cerevisiae* cell cycle. *J. Cell Biol.* 107: 1409–1426.

Jones, H. D., M. Schliwa, and D. G. Drubin. 1993. Video microscopy of organelle inheritance and motility in budding yeast. *Cell Motil. Cytoskeleton.* 25:129–142.

Koning, A. J., P. Y. Lum, J. M. Williams, and R. Wright. 1993. DiOC6 staining reveals organelle structure and dynamics in living cells. *Cell Motil. Cytoskeleton.* 25:111–128.

Koonce, M. P., P. M. Grissom, and J. R. McIntosh. 1992. Dynein from *Dictyostelium:* primary structure comparisons between a cytoplasmic motor enzyme and flagellar dynein. *J. Cell Biol.* 119:1597–1604.

Li, Y.-Y., E. Yeh, T. S. Hays, and K. Bloom. 1993. Disruption of mitotic spindle orientation in a yeast dynein mutant. *Proc. Natl. Acad. Sci. USA.* 90:10096–10100.

Mitchison, T. J., and E. D. Salmon. 1992. Poleward kinetochore fiber movement occurs during both metaphase and anaphase A in newt lung cell mitosis. *J. Cell Biol.* 119:569–582.

Myers, A. M., A. Tzagoloff, D. M. Kinney, and C. J. Lusty. 1986. Yeast shuttle and integrative vectors with multiple cloning sites suitable for construction of lacZ fusions. *Gene (Amst.).* 45:299–310.

Palmer, R. E., M. Koval, and D. Koshland. 1989. The dynamics of chromosome movement in the budding yeast *Saccharomyces cerevisiae*. 109:3355–3366.

Palmer, R. E., D. S. Sullivan, T. C. Huffaker, and D. Koshland. 1992. Role of astral microtubules and actin in spindle migration and orientation in the budding yeast, *Saccharomyces cerevisiae*. *J. Cell Biol.* 119:583–593.

Paschal, B. M., E. L. F. Holzbaur, K. K. Pfister, S. Clark, D. I. Meyer, and R. B. Vallee. 1993. Characterization of a 50-kDa polypeptide in cytoplasmic dynein preparations reveals a complex with $p150^{GLUED}$ and a novel actin. *J. Biol. Chem.* 268:15318–15323.

Plamann, M., P. F. Minke, J. H. Tinsley, and K. S. Bruno. 1994. Cytoplasmic dynein and actin-related protein Arp1 are required for normal nuclear distribution in filamentous fungi. *J. Cell Biol.* 127:139–149.

Pringle, J. R., and L. H. Hartwell. 1981. The *Saccharomyces cerevisiae* cell cycle. *In* The Molecular Biology of the Yeast *Saccharomyces.* Life cycle and inheritance. J. N. Strathern, E. W. Jones, and J. R.. Broach, editors. Cold Spring Harbor Laboratory, Cold Spring Harbor, NY. 97–142.

Pringle, J. R., R. A. Preston, A. E. M. Adams, T. Stearns, D. G. Drubin, B. Haarer, and E. W. Jones. 1989. Fluorescence microscopy methods in yeast. *Methods Cell Biol.* 31:357–435.

Salmon, E. D. 1989. Microtubule dynamics and chromosome movement. *In* Mitosis: Molecules and Mechanisms. Hyman and Brinkley, editors. Academic Press Limited, London. 119–181.

Salmon, E. D., T. Inoue, A. Desai, and W. Murray. 1994. High resolution multimode digital imaging system for mitosis studies *in vivo* and *in vitro*. *Biol. Bull.* 187:231–232.

Saunders, W. S., D. Koshland, D. Eshel, I. R. Gibbons, and M. A. Hoyt. 1995. S. cerevisiae kinesin- and dynein-related proteins required for anaphase chromosome segregation. *J. Cell Biol.* 128:617–624.

Schroer, T. A. 1994. New insights into the interaction of cytoplasmic dynein with the actin-related protein, Arp1. *J. Cell Biol.* 127:1–4.

Sherman, F., G. R.. Fink, and J. B. Hicks. 1986. Methods in Yeast Genetics. Cold Spring Harbor Press, Cold Spring Harbor, NY.

Skibbens, R. V., V. P. Skeen, and E. D. Salmon. 1993. Directional instability of kinetochore motility during chromosome congression and segregation in mitotic newt lung cells: a push-pull mechanism. *J. Cell Biol.* 122:859–875.

Sullivan, D. S., and T. C. Huffaker. 1992 Astral microtubules are not required for anaphase B in *Saccharomyces cerevisiae*. *J. Cell Biol.* 119:379–388.

Thomas, J. H., and D. Botstein. 1986. A gene required for the separation of chromosome on the spindle apparatus in yeast. *Cell.* 44:65–76.

Vallen, E. A., T. Y. Scherson, T. Roberts, K. van Zee, and M. D. Rose. 1992. Asymmetric mitotic segregation of the yeast spindle pole body. *Cell.* 69:505–515.

Walker, R. A., N. R. Gliksman, and E. D. Salmon. 1990. Using video-enhanced differential interference contrast microscopy to analyze the assembly dynamics of individual microtubules in real time. *In* Optical Microscopy for Biology. B. Herman and K. Jacobson, editors. Wiley-Liss, Inc., NY. 395–407.

West, R. R., and J. R. McIntosh. 1993. Characterization of cytoplasmic dynein in fission yeast. *Mol. Biol. Cell. Suppl.* 4:46a.

Winey, M., M. A. Hoyt, C. Chan, L. Goetsch, D. Botstein, and B. Byers. 1993. *NDC1*: a nuclear periphery component required for yeast spindle pole body duplication. *J. Cell Biol.* 122:743–751.

Xiang, X., S. M. Beckwith, and N. R. Morris. 1994. Cytoplasmic dynein is involved in nuclear migration in *Aspergillus nidulans*. *Proc. Natl. Acad. Sci. USA.* 91:2100–2104.